

# Using gas-phase nitric acid as an indicator of PSC composition

Miriam von König, Holger Bremer, Armin Kleinböhl, Harry Küllmann and Klaus F. Künzi  
Institute of Environmental Physics, University of Bremen, Bremen, Germany

Albert P. H. Goede

Space Research Organisation of the Netherlands (SRON), Utrecht, The Netherlands

Edward V. Browell and William B. Grant

Atmospheric Sciences Research, NASA Langley Research Center, Hampton, Virginia, USA

John F. Burris, Thomas J. McGee and Laurence Twigg

NASA Goddard Space Flight Center, Greenbelt, Maryland, USA

## Abstract

The composition of polar stratospheric cloud particles is investigated using data from several remote sensing instruments: gas-phase  $\text{HNO}_3$  measured by the Airborne Submillimeter Radiometer ASUR, temperature measured by the Airborne Raman Ozone, Temperature and Aerosol Lidar AROTEL, and aerosol backscatter wavelength dependence and depolarisation measured by the UV Differential Absorption Lidar DIAL. All three instruments have been operated onboard the NASA DC-8 during the SOLVE winter 1999/2000. A simple thermodynamical model is used to calculate the gas-phase amount of  $\text{HNO}_3$  in the presence of polar stratospheric clouds along the flight-track of the DC-8 for one flight into the polar vortex on December 7, 1999. Three types of PSCs are considered in the model: Nitric acid trihydrate (NAT), nitric acid dihydrate (NAD) and supercooled ternary solutions (STS). The comparison of the modeled and measured gas-phase  $\text{HNO}_3$  in the presence of PSCs shows a very good agreement if a NAT composition of the particles is assumed. However, sensitivity studies show that while the PSCs observed on this flight are not in agreement with a STS composition, the model is very sensitive to temperature, and a NAD composition of the PSC cannot be ruled out.

## Introduction

Polar stratospheric clouds (PSCs) have been known to play a crucial role in stratospheric Arctic and Antarctic winter/spring ozone depletion for a long time (see e.g. [Peter, 1997; Solomon et al., 1999]). The heterogeneous reactions leading to chlorine activation, a prerequisite of ozone depletion, take place on the surfaces of solid stratospheric particles or in liquid stratospheric particles. These reactions convert chlorine reservoir species like  $\text{ClONO}_2$  and  $\text{HCl}$  into reactive and easily photolyzed species that can participate in catalytic ozone depletion cycles, and also form  $\text{HNO}_3$  condensed in the particles and lead to an increase of the gas-phase amount of  $\text{HNO}_3$  when the PSC evaporates.

PSCs are known to appear in two major compositions: below the ice frost point, ice particles will form (Type II PSCs). Type I PSCs form some Kelvin above the ice frost point and are believed to be condensates of  $\text{HNO}_3$  and water. While the formation of Type II PSCs seems reasonably well understood, a considerable amount of uncertainty exists concerning the formation, as well as the composition, of Type I PSCs. Type I PSCs exist as solid condensates of  $\text{HNO}_3$  and water (Type Ia), as well as in the form of supercooled ternary solutions of  $\text{HNO}_3$ ,  $\text{H}_2\text{O}$  and  $\text{H}_2\text{SO}_4$  (Type Ib), formed by cooling of the background aerosol [Carslaw et al., 1994; Tabazadeh et al., 1994]. Type Ia PSCs have first been suggested to be composed of nitric acid trihydrate NAT,  $\text{HNO}_3 \cdot 3\text{H}_2\text{O}$  [Hanson and Mauersberger, 1988]. However, the formation of NAT particles still poses many unanswered questions. Different possibilities for the composition of PSC Type Ia have been proposed by some authors. For example, Worsnop et al. [1993] proposed nitric acid dihydrate (NAD,  $\text{HNO}_3 \cdot 2\text{H}_2\text{O}$ ) as a possible composite for Type Ia PSCs.

All PSC composites – ice, STS and NAT or NAD – not only form at different temperatures, but also support different reaction rates of chlorine activation and denoxification reactions. Therefore, the composition of the PSCs will not only determine the temperature below which chlorine activation occurs, but also the lifetime of the chlorine reservoir species in the presence of PSCs. Thus, to know the composition and formation mechanism of PSC particles is a prerequisite to model ozone depletion accurately and to predict possible future ozone depletion. This is especially true for the Arctic winter, where temperatures are rarely below the ice frost point, and even temper-

atures below the NAT threshold occur infrequently and for shorter periods of time than in the Antarctic winter [WMO, 1999; Pawson and Naujokat, 1999].

Considering the importance of PSC composition for the determination of ozone depletion, very few direct measurements exist. The bulk of PSC measurements consist of measuring optical properties – i.e., particle backscatter wavelength dependence and depolarisation. The first ever direct measurement of PSC composition occurred as late as 1998, with a balloon borne mass spectrometer [Schreiner et al., 1999]. This instrument is to date the only instrument able to measure directly the composition of PSCs. It has flown successfully several times since 1998, most prominently during the SOLVE/THESEO 2000 campaign [Voigt et al., 2000a,b].

We present an indirect method to determine the composition of Type I PSCs from a combination of gas-phase  $\text{HNO}_3$  mixing ratios measured by the Airborne Submillimeter Radiometer (ASUR), temperature measurements obtained by the Airborne Raman Ozone, Temperature and Aerosol Lidar (AROTEL) (McGee et al., manuscript in preparation), and PSC backscatter wavelength dependence and depolarisation measured by the UV Differential Absorption Lidar (DIAL) to identify the PSC boundaries [Browell et al., 1983; 1998]. A first approach to determine the PSC composition from the gas-phase amount of  $\text{HNO}_3$  was presented already in 1990 [Schreiner and Arnold, 1990], using one  $\text{HNO}_3$  profile measured by a rocket-borne instrument. Recently, Santee et al. [2001] used a combination of satellite measurements – POAM particle scattering and MLS  $\text{HNO}_3$  profiles – to study PSC types and PSC formation during the Arctic winter 1995/96. While satellite measurements have the advantage of greater coverage, the ASUR, DIAL and AROTEL measurements have been obtained with a very good horizontal resolution, which makes it possible to study the structure of individual PSCs.

## Measurement of gas-phase $\text{HNO}_3$

$\text{HNO}_3$  was measured by the Airborne Submillimeter Radiometer ASUR. ASUR was developed for airborne measurements of stratospheric trace gases at the University of Bremen, in collaboration with the Space Research Organisation of the Netherlands (SRON). It was flown for the first time during the EASOE campaign in winter 1991/92 [Crewell et al., 1994]. It has been improved continuously and has

participated in a number of measurement campaigns during several Arctic winters [e.g. Wehr et al., 1995; Crewell et al., 1995; de Valk et al., 1997; von König et al., 2000]. Implementation of a liquid helium cooled SIS diode as the detector in 1994 has improved the signal-to-noise ratio by about a factor of fifteen [Mees et al., 1995]. The frequency range has been extended several times, increasing the number of measurable species. ASUR now covers the complete frequency range from 604.3 GHz to 662.3 GHz. This range includes lines of ClO, HCl, O<sub>3</sub>, N<sub>2</sub>O, HO<sub>2</sub>, BrO, CH<sub>3</sub>Cl, H<sub>2</sub>O and HNO<sub>3</sub>. However, since the instrument's instantaneous bandwidth is about 1.5 GHz, not all species can be measured simultaneously.

The lines measured are transitions from thermally excited rotational states, so measurements can be conducted independent of solar zenith angle. Measurements are affected solely by gas-phase species, not by solid or liquid phases. At the measured wavelength of about 0.5 mm, measurements are not affected by scattering from stratospheric particles. Cloud particles will contribute to the continuum radiation due to their broad-band thermal emission. This can lead to an increase of the background radiation and therefore to a broad-band absorption of stratospheric species for large visible cirrus clouds [Bühler et al., 1999]; however, optically thin clouds with small particles or small particle densities like Type I PSCs will not affect the measurement significantly.

During the SOLVE/ THESEO 2000 campaign, the instrument was mounted on the starboard side of the NASA DC-8 aircraft, measuring with a fixed elevation angle of 12 degrees.

The pressure broadening of the lines is used to derive altitude information from the measurements. Measured spectra are analyzed using the Optimal Estimation Method described in detail e.g. in Rodgers [1976; 1990]. For HNO<sub>3</sub>, vertical profiles of volume mixing ratio are retrieved on a 2 km altitude grid using a zero a priori profile. This leads to very smooth profiles with an altitude resolution of 6-10 km in the lower stratosphere, with the resolution decreasing to higher altitudes (see e.g. [Kleinböhl et al., 2001]). Spectra are integrated over approximately 100 s to achieve a sufficient signal-to-noise ratio. This leads to a horizontal resolution of about 20 km and a precision of about 0.3 ppb in the lower stratosphere. Sensitivity studies have been carried out to investigate the influence of systematic errors on the measurement. Several sources of possible systematic errors have been considered. The dominant source of

systematic errors was found to be the influence of nearby ozone lines and the calculation of the continuum, and an overall systematic error of 15 % or 0.6 ppb – whichever is larger – was estimated for the measurement accuracy. This value is confirmed by comparison with other HNO<sub>3</sub> profile measurements, e.g. with the MIPAS instrument and ground-based FTIR measurements [von König, 2001].

## Measurements of December 7, 1999

In this paper, we focus on measurements from one flight during the first SOLVE deployment. On December 7, 1999, a flight was carried out to the Arctic islands of Franz-Josef-Land, Severnaya Semlja, and Spitzbergen. Around and north-east of Severnaya Semlja, a triangle was flown (see Figure 1). Temperatures had just fallen below the PSC threshold in the core of the polar vortex; the aim of this flight was to search for PSCs in the cold core of the polar vortex. Temperature measurements along the flight-track of the DC-8 show very low stratospheric temperatures during most of this flight (see Figure 2 A). Two PSCs were observed during this flight by the DIAL lidar (see Figure 2 B). These PSCs were observed during the first and third leg of the triangle as well as during the first part of the second leg, extending from 18 km to 24 km in altitude and over a horizontal range of several hundreds of kilometers. Both PSCs were identified by their optical properties as Type Ia PSCs, i.e. solid particles presumed to be NAT. Both show a similar, very distinct vertical structure, so it is safe to assume that this was the same cloud, crossed twice. HNO<sub>3</sub> was measured regularly by ASUR during this flight, with only short interruptions to tune to other molecules. A clear anticorrelation is observed between the lidar backscatter measurements and the ASUR HNO<sub>3</sub> measurements. During the PSC crossings, the gas-phase HNO<sub>3</sub> observed by ASUR decreases by more than 2 ppb (Figure 2 C). Due to the restricted vertical resolution of ASUR, the vertical structure of the PSC is not reflected in the HNO<sub>3</sub> measurements. Rather, the decrease of HNO<sub>3</sub> is observed over a large vertical range from 17 km to 26 km.

## Model

### Model description

A simple model was developed to calculate gas-phase HNO<sub>3</sub> mixing ratios in thermodynamical equi-

librium for three types of PSCs: nitric acid trihydrate, NAT, nitric acid dihydrate, NAD and super-cooled ternary solutions, STS. All three types consist of condensates of  $\text{HNO}_3$  and water. Gas-phase mixing ratios were derived from the vapor pressures of the condensates. For the solid condensates, the  $\text{HNO}_3$  equilibrium mixing ratio is a function of temperature, pressure and water vapor. The gas-phase equilibrium mixing ratio of the liquid depends on all major contents of the liquid, i.e. on  $\text{H}_2\text{SO}_4$  and the amount of total  $\text{HNO}_3$  as well as on temperature, pressure and water vapor. Total  $\text{HNO}_3$  means the sum of gas-phase and condensed  $\text{HNO}_3$ . The  $\text{HNO}_3$  mixing ratio for NAT was calculated according to Hanson and Mauersberger [1988], for NAD according to Worsnop et al. [1993], and for STS according to Carslaw et al. [1995].

Temperature and density were measured by the AROTEL lidar operating onboard the DC-8 [Burris et al., 2001]. Water vapor was assumed to increase from 4.75 ppm at about 60 hPa to 6.25 ppm at about 20 hPa altitude, in agreement with balloon measurements obtained during the SOLVE campaign [Schiller et al., 2001]. Values of total  $\text{HNO}_3$  were estimated from ASUR measurements outside PSCs, taken during the same flight well inside the polar vortex. No measurements of  $\text{H}_2\text{SO}_4$  were available. A  $\text{H}_2\text{SO}_4$  value of 0.5 ppb was assumed, in agreement with values estimated by [Beyerle et al., 1997] for low aerosol loading. A summary of the model parameters and their values or sources is given in Table 1.

Model calculations were carried out for all locations where PSCs were observed by DIAL. PSC observations were defined by aerosol backscatter ratios larger than 0.6 in the infrared channel of the DIAL instrument. To minimize the influence of measurement noise, only grid-points for which the running mean of three neighbouring grid-points had IR aerosol backscatter ratios larger than 0.6 were used. This procedure yields model values of the  $\text{HNO}_3$  mixing ratio with the vertical spacing of the DIAL data (about 75 m), and the horizontal resolution of the DIAL data, as well. Both the vertical resolution and the horizontal resolution of the DIAL data is much higher than that of the ASUR data, so the model calculations have a better resolution than the ASUR measurements. To make these model profiles comparable to the measured  $\text{HNO}_3$  values, the model profiles were embedded into the total  $\text{HNO}_3$  profile extending from 10 km to 50 km altitude and smoothed to the ASUR altitude resolution. The model results were

not smoothed horizontally. The subsequent steps of the model calculation and smoothing are shown in Figure 3 for the example of NAT.

It should be noted that the formation of NAT as well as NAD was thermodynamically possible in some situations where no PSCs could be identified by the lidar data. No model calculations were carried out for those situations.

### Model results and comparison with measurements

In Figure 3, the results of the model calculation are shown for the high-resolution profiles as well as for the model profiles on ASUR resolution for the example of NAT. Model results are shown over an altitude range of 16 km to 26 km, and are compared to the measured  $\text{HNO}_3$  values over the same altitude range. In the high-resolution model run (Figure 3 A),  $\text{HNO}_3$  values decrease from over 9.5 ppb to values of less than 1.5 ppb. The smoothed model profiles show a distinctive lower  $\text{HNO}_3$  decrease (Figure 3 B). Values decrease from over 9.5 ppb outside the PSC to over 7.25 ppb during the first PSC observation, and over 6 ppb during the second PSC observation. The vertical structure is no longer reflected in the model profiles. Indeed, the smoothed model profiles for NAT show values and a horizontal variability very much like the measured  $\text{HNO}_3$  (Figure 3 C), with very little vertical structure.

As both the modeled and measured smoothed profiles show very little vertical structure, mixing ratios from anywhere between 18 km and 24 km altitude show a similar behavior. In the following, only values from 22 km altitude are shown. It should be noted, however, that values from 18, 20 or 24 km altitude show a consistent behavior. In Figure 4, the evolution of the  $\text{HNO}_3$  mixing ratio at 22 km altitude is shown during the PSC underflights. Shown are deviations from total  $\text{HNO}_3$  for the measured values as well as for smoothed model results for NAT, NAD and STS. As already seen in Figure 3, the model results for NAT are in fairly good agreement with the measurement over large parts of the PSCs. Significant discrepancies between measurement and model only occur at the beginning of the second PSC underflight, where the modeled  $\text{HNO}_3$  starts to decrease earlier than the measured  $\text{HNO}_3$ . The model results for NAD show significantly less variability than the measurement over most parts of the PSC observations. Only at the end of the first PSC observation and at the beginning of the second PSC observation

– where the agreement with NAT is worst – the modeled  $\text{HNO}_3$  for NAD is in reasonable agreement with the measurements. The model results for STS show practically no variation during the complete modeled period; temperatures were apparently not low enough for the formation of STS.

A problem in the comparison of measurements and model results could be the spatial offset between the ASUR and the lidar line-of-sight. While the lidar observes in a zenith looking geometry, ASUR measures with a  $12^\circ$  elevation angle. This leads to a spatial offset of about 40 to 60 km at the altitudes where particles were observed. However, the PSC observed on this day was very large; the legs during which particles were observed above the airplane cover an area of about 188,000 sq km, about half the size of Germany. The spatial offset should play a role mainly at the edges of the PSC, at the beginning and at the end of the PSC underflights. However, as the PSC was crossed clockwise and ASUR is mounted to the right side of the airplane, the ASUR instrument always looked further into the PSC than the lidar. So, spatial offset cannot explain the discrepancies between measured and modeled  $\text{HNO}_3$  at the beginning of the second PSC underflight.

Another point to consider in this comparison is the assumption of equilibrium. While liquid particles form comparatively rapidly, solid particles like NAT and NAD can take several days to grow to their equilibrium size, and equally take some time to melt when temperatures rise. So particles are assumed to be smaller than their equilibrium size when the temperature is falling - and then the decrease of the gas-phase  $\text{HNO}_3$  is lower than for the equilibrium case -, but when temperatures are rising, the particles could actually be larger than their equilibrium size would be. Trajectory calculations using ECMWF wind fields and temperatures on the 435 K, 475 K and 550 K isentrope show that temperatures have been constant or falling for at least four days prior to the measurements, so this PSC was either in equilibrium or growing. That means that the equilibrium case is a limit for the gas-phase decrease: the particles are smaller or equal to the equilibrium case, but certainly not larger.

### Model sensitivity

The comparison of measured and modeled  $\text{HNO}_3$  shows a reasonably good agreement assuming a NAT composition of the PSC. This is consistent with the lidar measurements which already have shown that

the PSC is not liquid. How significant is this result? Can we conclude from these results that the PSC is composed of NAT? To investigate this, the sensitivity of the model is tested for the parameters used as input for the calculation of gas-phase  $\text{HNO}_3$ : Temperature,  $\text{H}_2\text{O}$ , total  $\text{HNO}_3$  and  $\text{H}_2\text{SO}_4$ .

**Temperature.** Temperature was measured by the AROTEL instrument using Raman scattering. As the observed PSCs are optically thin, measurements are not affected by scattering on the PSC particles. The measurement error of the AROTEL measurements range from less than 1 K to values above 3 K, and generally increases with altitude (Figure 5). Here, the temperature error of the individual measurements was used.

**$\text{H}_2\text{O}$ .**  $\text{H}_2\text{O}$  values are estimated from several balloon measurements taken during the SOLVE campaign [Schiller et al., 2001]. While qualitatively all measurements agree quite well, differences of up to 0.4 ppm are observed between the measurements. All  $\text{H}_2\text{O}$  measurements discussed in Schiller et al. [2001] are cited to be obtained in vortex situations similar to those of the December 7, 1999, flight, i.e. they were obtained either 'inside the polar vortex' or 'deep inside the polar vortex'. However, those measurements were all carried out near Kiruna in Northern Sweden, quite a large distance from the measurements discussed here. An error of 1 ppm is considered here for water vapor to account for variabilities due to the different measurement sites.

**$\text{HNO}_3$ .** Total  $\text{HNO}_3$  contributes to the model result in two ways: The gas-phase equilibrium mixing ratio of STS depends on total  $\text{HNO}_3$ ; further, total  $\text{HNO}_3$  is used for the smoothing of the high-resolution model profiles. Values of total  $\text{HNO}_3$  are estimated from ASUR measurements outside of PSCs, but inside the vortex. The accuracy of the ASUR measurements is about 15 % (see instrument description). A further error source could be the low vertical resolution of the measured  $\text{HNO}_3$  profiles. This could pose a serious problem if the  $\text{HNO}_3$  profiles were strongly structured, as during a PSC underflight or in situations with significant denitrification. As it was rather early in the winter, denitrification is very unlikely to have occurred at that time. To quantify the influence of vertical resolution on the model results, model runs were carried out using three different profiles with different altitude resolutions. All three profiles give essentially the same profile if smoothed to the altitude resolution of the ASUR measurement. The unsmoothed profiles, however, show different peak altitudes, peak

values and peak width (see Figure 6 A). The profiles were chosen to display a wide range of peak values and peak altitudes that agree with the ASUR measurement without PSC coverage when folded to the ASUR vertical resolution. The model results for the three different profiles are shown for the case of NAT in Figure 6 B. No significant differences can be observed between the three model runs, so the vertical resolution of the total  $\text{HNO}_3$  profile is assumed not to contribute significantly to the model errors. A model error of 15 % is assumed for total  $\text{HNO}_3$ .

**$\text{H}_2\text{SO}_4$ .** No measurements were available for sulphuric acid mixing ratios. A value of about 0.5 ppb was assumed, varied between 0.3 ppb and 1.1 ppb to match the limits of the values given by Beyerle et al. [1997] for the altitude range of the PSC (approx. 430 to 540 K). These variations had no substantial influence on the model results. It should be noted that the values of Beyerle et al. [1997] used for this estimate were obtained in Winter 1992/1993, when the aerosol loading might still have been influenced by the eruption of mount Pinatubo two years previous, so the  $\text{H}_2\text{SO}_4$  values could be systematically too high. However, assuming lower  $\text{H}_2\text{SO}_4$  values does not change the model results, as the lowest value derived from Beyerle et al. [1997] is already too low for the formation of liquid aerosols at these temperatures.

A summary of the estimated uncertainties of the model parameters is given in Table 1. Model runs have been conducted for all three types of PSCs, changing the input parameters by the estimated uncertainties. The model uncertainties due to individual input parameters were calculated as the deviations of these model runs to the initial run, and a total model error was calculated as the root mean square of all the individual model errors. Total model errors are shown in Figure 7 A-C, together with the model results, compared to the measurements. Even considering the total model errors, the PSC is not consistent with a STS composition (Figure 7 C). This result is in good agreement with the lidar measurements. A similarly clear distinction between a NAT and NAD composition is not possible. Considering the total errors, most of the PSC could be either NAT or NAD.

What causes these large model errors? The dark grey areas in Figure 7 show the sum of the model errors *without the temperature uncertainties*. Now the errors are much smaller, in the range of, or even smaller than, the precision of the ASUR measurements. So, by far the largest contribution to the model errors come from uncertainties in the temper-

ature data. In Figure 8, model results and errors are plotted assuming a temperature error of 1K. Now, a distinction between NAT and NAD would be possible in most parts of the PSC. It follows that temperature data with an accuracy of better than 1 K are necessary to distinguish between the gas-phase  $\text{HNO}_3$  amounts of NAT and NAD.

On the other hand, this PSC was probably not in equilibrium, but growing, so the equilibrium values are a limit for the gas-phase decrease; considering this, the PSC is unlikely to be NAD, as the measured gas-phase decrease is larger than the model result for NAD in most places.

## Summary and conclusions

The aim of this paper is to investigate the composition of polar stratospheric cloud particles using a combination of gas-phase  $\text{HNO}_3$  measurements and lidar data. Data from one research flight of the DC-8 into the polar vortex carried out on December 7, 1999, were used for the investigation. Measurements of gas-phase  $\text{HNO}_3$  were provided by the Airborne Submillimeter Radiometer ASUR; simultaneous measurements of aerosol backscatter wavelength dependence and depolarisation by the UV DIAL lidar were used to identify the boundaries of polar stratospheric clouds. Two PSCs of Type Ia were observed by the lidar during this flight, and both PSC observations were correlated with a decrease of gas-phase  $\text{HNO}_3$ .

Model runs were carried out for three different compositions of Type I PSCs – NAT, NAD and STS – using temperature data measured by the Airborne Raman Ozone, Temperature and Aerosol Lidar AROTEL. Sensitivity studies for the model input parameters – temperature,  $\text{H}_2\text{O}$ , total  $\text{HNO}_3$  and  $\text{H}_2\text{SO}_4$  – were carried out, and the influence of the limited altitude resolution of the total  $\text{HNO}_3$  profile was investigated. The smoothing of the total  $\text{HNO}_3$  profile was shown to have little influence on the model results. Systematic errors of  $\text{H}_2\text{O}$ ,  $\text{H}_2\text{SO}_4$  and total  $\text{HNO}_3$  add up to a model error of about 0.4 ppb, in the order of magnitude of the measurement precision. A far larger impact on the model errors comes from temperature uncertainties.

Comparison of the model runs with the measured  $\text{HNO}_3$  shows that these PSCs are in good agreement with a NAT composition, while NAD and especially STS compositions of the PSCs lead to a lower  $\text{HNO}_3$  decrease over large parts of the PSC observations. Considering the estimated model errors, it is possi-

ble to show with these measurements that the PSCs are not composed of STS, in agreement with the lidar data which show that the PSCs contain solid particles. However, considering the model errors, a NAD composition of the particles cannot be ruled out. On the other hand, considering non-equilibrium formation of solid PSCs leads to the conclusion that the PSCs were probably growing, and were found much more likely to be NAT than NAD.

It was demonstrated in this paper that gas-phase measurements of  $\text{HNO}_3$  can provide valuable information about the PSC composition additional to lidar measurements; however, for different meteorological situations - for melting PSCs and rapidly forming wave-PSCs - the non-equilibrium composition of solid particles will pose a problem. A way around the problem of non-equilibrium could be to use the lidar data to calculate the microphysical properties of the particles - particle density, size distribution and condensed mass - as shown e.g. in the paper of Hu et al. [2001], and calculate the condensed mass, condensed  $\text{HNO}_3$  and gas-phase decrease of  $\text{HNO}_3$  from these measurements.

#### Acknowledgments.

We would like to thank G. Nèveke for technical support before and during the campaign, and the aircraft crew for their excellent support. We would also like to thank NASA for the opportunity to participate onboard the DC-8. The campaign participation was funded by the European Union (contract EVK2-CT-1999-00047).

#### References

- Beyerle, G., Luo, B., Neuber, R., Peter, Th. and McDermid, I.S., Temperature dependence of ternary solution particle volume as observed by lidar in the Arctic stratosphere during winter 1992/1993, *J. Geophys. Res.*, 102, 3603-3609, 1997.
- Browell, E.V., A.F. Carter, S.T. Shipley, R.J. Allen, C.J. Butler, M.N. Mayo, J.H. Siviter Jr., and W.M. Hall, NASA multipurpose airborne DIAL system and measurements of ozone and aerosol profiles, *Appl. Opt.* 22, 522-534, 1983.
- Browell, E.V., S. Ismail, and W.B. Grant, Differential Absorption Lidar (DIAL) measurements from air and space, *Appl. Phys. B*, 67, 399-410, 1998.
- Bühler, S., von Engel, A., Urban, J., Wohlgenuth, J., und Künzi, K.F., The impact of cirrus clouds, *ESTEC technical report, Contract No 12053*, 1999.
- Burris, J., McGee, T., Hoegy, W., Lait, L., Twigg, L., Sumnicht, G., Hostetler, C., Bui, T.P., Neuber, R., McDermid, I.S., Validation of Temperature Measurements from the Airborne Raman Ozone, Temperature and Aerosol Lidar During SOLVE, *J. Geophys. Res., this issue*, 2001.
- Carlsaw, K.S., B.P. Luo, S.L. Clegg, Th. Peter, P. Brimblecombe, and P.J. Crutzen, Stratospheric aerosol growth and  $\text{HNO}_3$  gas phase depletion from coupled  $\text{HNO}_3$  and water uptake by liquid particles, *Geophys. Res. Lett.*, 21, 2479-2482, 1994.
- Carlsaw, K.S., B. Luo, and T. Peter, An analytic expression of aqueous  $\text{HNO}_3$ - $\text{H}_2\text{SO}_4$  stratospheric aerosols including gas phase removal of  $\text{HNO}_3$ , *Geophys. Res. Lett.*, 14, 1877-1880, 1995.
- Crewell, S., P. Hartogh, K.F. Künzi, H. Nett, and T. Wehr, Aircraft measurements of ClO and HCl during EASOE 1991/92, *Geophys. Res. Lett.*, 21, 1267-1279, 1994.
- Crewell, S., R. Fabian, K.F. Künzi, H. Nett, W. Read, J. Waters, and T. Wehr, Comparison of ClO measurements by airborne and spaceborne microwave radiometers in the Arctic winter stratosphere 1993, *Geophys. Res. Lett.*, 22, 1489-1492, 1995.
- Hanson, D., and K. Mauersberger, Laboratory studies of the nitric acid trihydrate: Implications for the south polar stratosphere, *Geophysical Research Letters* 15, 855-858, 1988.
- Hu, R.-M., K.S. Carlsaw, C. Hostetler, L. R. Poole, B. Luo, Th. Peter, S. Fuglistaler, T.J. McGee, and J.F. Burris, The microphysical properties of wave PSCs retrieved from lidar measurements during SOLVE / THESEO 2000, *J. Geophys. Res.*, this issue, 2001.
- Kleinböhl, A., et al., Vortexwide Denitrification of the Arctic Polar Stratosphere in Winter 1999/2000 determined by Remote Observations, *J. Geophys. Res.*, this issue, 2001.
- Mees, J., S. Crewell, H. Nett, G. de Lange, H. van den Stadt, J.J. Kuipers, and R.A. Panhuyzen, ASUR - An Airborne SIS receiver for Atmospheric Measurements of Trace Gases at 625 to 760 GHz, *IEEE Transactions on Microwave Theory and Techniques*, 43, 1995.
- Pawson, S., and Naujokat, B., The cold winters of the middle 1990s in the northern lower stratosphere, *J. Geophys. Res.*, 104, 14209-14222, 1999.
- Peter, T., Microphysics and heterogeneous chemistry of polar stratospheric clouds, *Annual Rev. of Phys. Chem.*, 48, 785-822, 1997.
- Rodgers, C.D., Retrieval of atmospheric temperature and composition from remote measurements of thermal radiation, *Rev. of Geophys. and Space Physics* 14, 609-624, 1976.
- Rodgers, C.D., Characterization and error analysis of profile retrieval from remote sounding measurements, *J. Geophys. Res.*, 95, 5587-5595, 1990.
- Santee, M., A. Tabazadeh, G.L. Manney, M.D. Fromm, R.M. Bevilacqua, J.W. Waters, and E.J. Jensen, A Lagrangian approach to inferring the composition of Arctic polar stratospheric clouds from UARS MLS  $\text{HNO}_3$  and POAM II aerosol extinction measurements submit-

- ted to *J. Geophys. Res.*, 2001.
- Schiller, C., et al., Dehydration in the Arctic stratosphere during the THESEO 2000/SOLVE campaigns, *J. Geophys. Res.*, in press, 2001.
- Schlager, H., and F. Arnold, Measurement of stratospheric gaseous nitric acid in the Winter arctic vortex using a novel rocket-borne mass spectrometer method, *Geophysical Research Letters* 17, 433-436, 1990.
- Schreiner, J., C. Voigt, A. Kohlmann, F. Arnold, K. Mauersberger and N. Larsen, Chemical analysis of polar stratospheric cloud particles, *Science* 283, 968-970, 1999.
- Solomon, S., Stratospheric ozone depletion: A review of concepts and history, *Rev. of Geophys.*, 37, 275-316, 1999.
- Tabazadeh, A., R.P. Turco, and M.Z. Jacobson, A model for studying the composition and chemical effects of stratospheric aerosols, *J. Geophys. Res.*, 99, 12897-12914, 1994.
- de Valk, J.P.J.M.M., et al., Airborne Heterodyne Measurements of stratospheric ClO, HCl, O<sub>3</sub> and N<sub>2</sub>O during SESAME-I over Northern Europe, *J. Geophys. Res.*, 102, 1391-1398, 1997.
- Voigt, C., et al., Nitric Acid Trihydrate in Polar Stratospheric Cloud Particles, *Science* 290, 1756, 2000a.
- Voigt, C., A. Tsias, A. Dörnbrack, S. Meillinger, B. Luo, J. Schreiner, N. Larsen, K. Mauersberger, Non-equilibrium compositions of ternary polar stratospheric clouds in gravity waves, *Geophys. Res. Lett.*, 27, 3873-3876, 2000b.
- von König, M., H. Bremer, V. Eyring, A. Goede, H. Hertzheim, Q. Kleipool, H. Küllmann, and K.F. Künzi, An airborne submm radiometer for the observation of stratospheric trace gases, in *Microwave Radiometry and Remote Sensing of the Earth's Surface and Atmosphere*, edited by P. Pampaloni and S. Paloscia, VSP Utrecht, 2000.
- von König, M., Chlorine Activation and PSC Formation in the Arctic Stratosphere, Ph.D. Thesis, University of Bremen, Bremen, Germany, 2001.
- Wehr, T., S. Crewell, K.F. Künzi, J. Langen, H. Nett, J. Urban, and P. Hartogh, Remote Sensing of ClO and HCl over Northern Scandinavia in Winter 1992 with an Airborne Submillimeter Radiometer, *J. Geophys. Res.*, 100, 20958-20968, 1995.
- World Meteorological Organisation, Scientific Assessment of Ozone Depletion: 1998, WMO Global Ozone Research and Monitoring Project Report 44, Geneva, 1999
- Worsnop, D.R., Fox, L.E., Zahniser, M.S., and Wofsy, S.C., Vapor Pressures of Solid Hydrates of Nitric Acid: Implications for Polar Stratospheric Clouds, *Science* 259, 71-74, 1993.
- von König, M., Bremer, H., Kleinböhl, A., Küllmann, H., and Künzi, K.F., Institute of Environmental Physics, University of Bremen, Kufsteiner Strasse, 28359 Bremen, Germany. (miriam@iup.physik.uni-bremen.de)
- A.P.H. Goede, Space Research Organisation of the Netherlands, Utrecht, The Netherlands.
- Browell, E. V., and Grant, W. B., NASA Langley Research Center, Atmospheric Sciences Research, MS 401A, VA 23681-2199, USA. (e.v.browell@larc.nasa.gov, w.b.grant@larc.nasa.gov)
- Burris, J. F., McGee, T. J., and Twigg, L., NASA Goddard Space Flight Center, Greenbelt, MD 20771, USA.

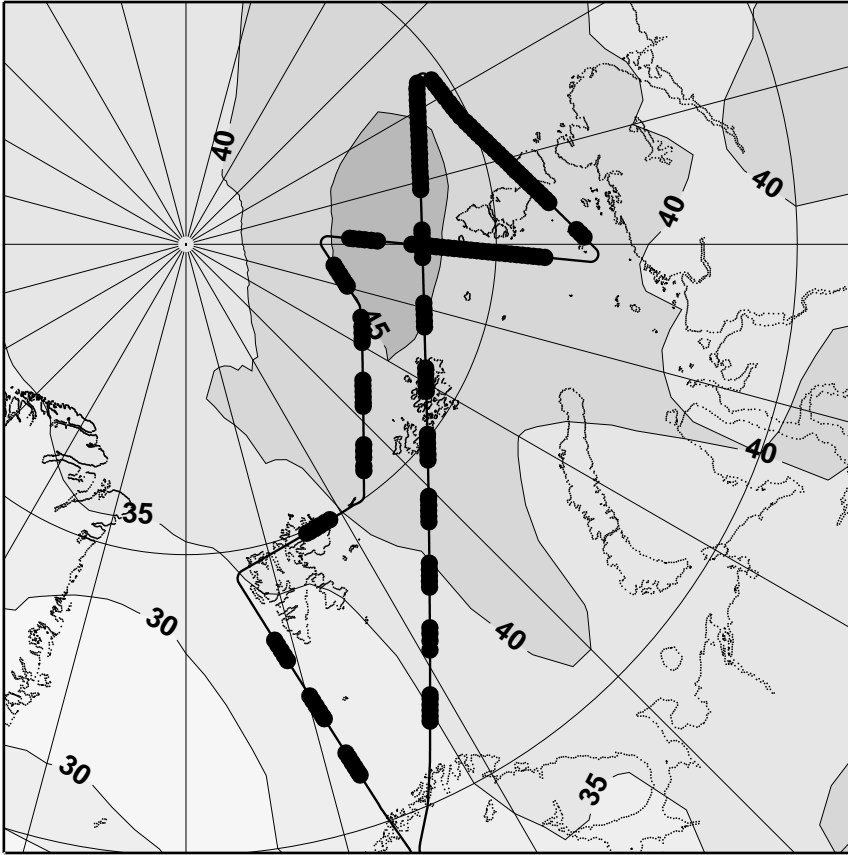


**Figure 1.** Flight track of the NASA DC-8 on December 7, 1999 (black line). Contours are ECMWF PV (in PVU) on the 475 K isentropic. Heavy black lines indicate portions of the flight where ASUR measured  $\text{HNO}_3$ . On the left hand side of the picture the coastline of north-east Greenland can be seen, coastlines in the bottom and right-hand side are the northern coast of Scandinavia and Siberia.

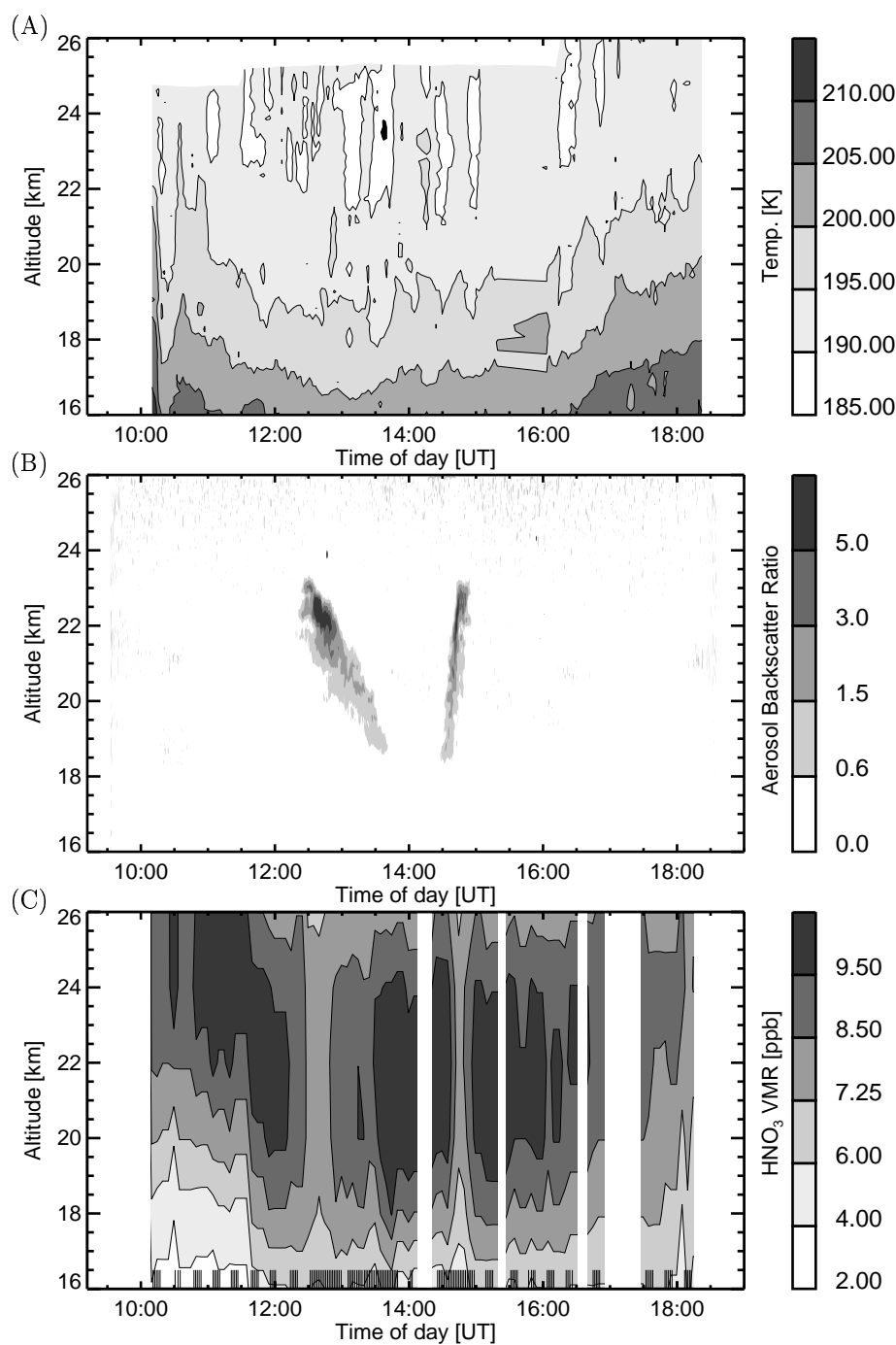


**Figure 2.** Top: Temperature along the flight path of the NASA DC-8 on December 7, 1999, measured by the AROTEL instrument. Middle: Aerosol backscatter ratio at  $1.06 \mu\text{m}$ , measured by the DIAL instrument during this flight. Two distinctive PSCs are observed, one from around 12:15 UT to around 13:45 UT, the other from 14:30 UT to around 15 UT. Bottom: Gas-phase HNO<sub>3</sub> mixing ratio measured by ASUR during the same flight. White spaces denote times when the ASUR instrument was tuned to other molecules. The measurements have been binned over five minute periods for greater clarity. Thin black lines at the bottom denote measurement positions of individual HNO<sub>3</sub> measurements. A decrease of gas-phase HNO<sub>3</sub> of more than 2 ppb is observed, clearly correlated to the lidar PSC observations.

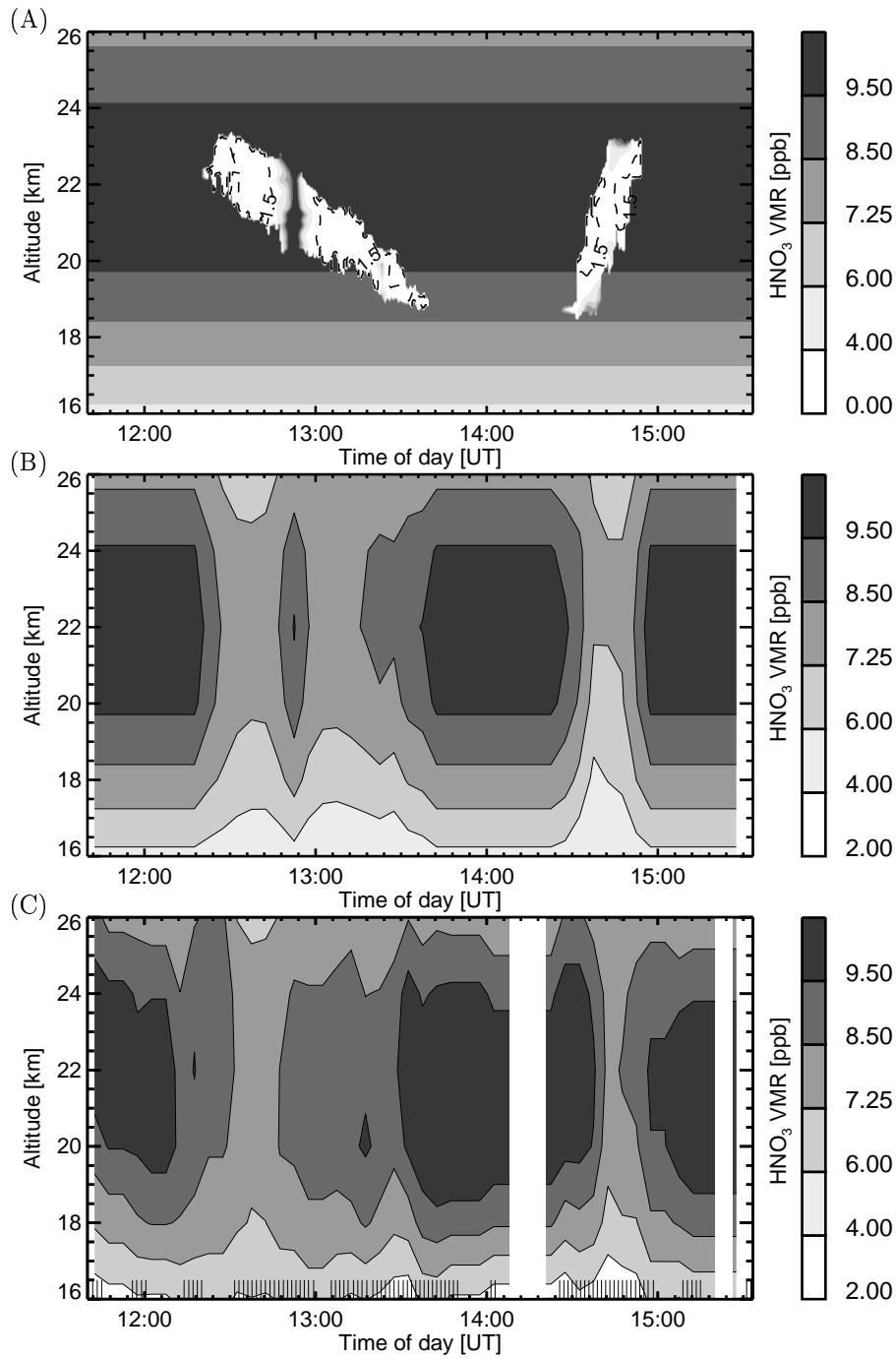


**Figure 3.** Model results for a NAT composition in comparison with measurements. Top: Calculated gas-phase mixing ratios of HNO<sub>3</sub> in equilibrium for a NAT composition, for all positions where PSCs were observed by DIAL. The HNO<sub>3</sub> values outside the PSC observations are total HNO<sub>3</sub> values derived from ASUR measurements without PSC coverage (see section Model description). Middle: the same model results, smoothed to ASUR's altitude resolution. Bottom: ASUR measurement of gas-phase HNO<sub>3</sub> along the same flight track. Measurements and smoothed model results have been binned over five minute periods for greater clarity.

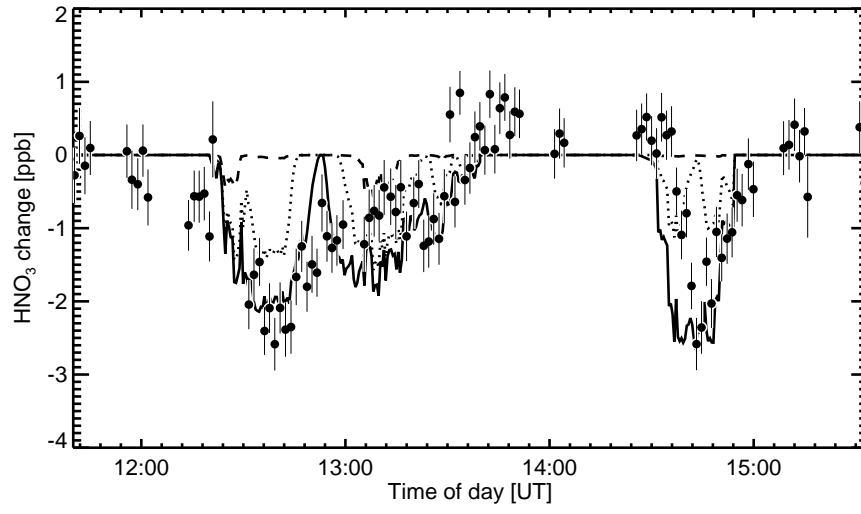


**Figure 4.** Model results for NAT (solid line), NAD (dotted line) and STS (dashed line) at 22 km altitude. Black dots are ASUR measurements at 22 km altitude. Error bars show the statistical  $1 \sigma$  measurement error.

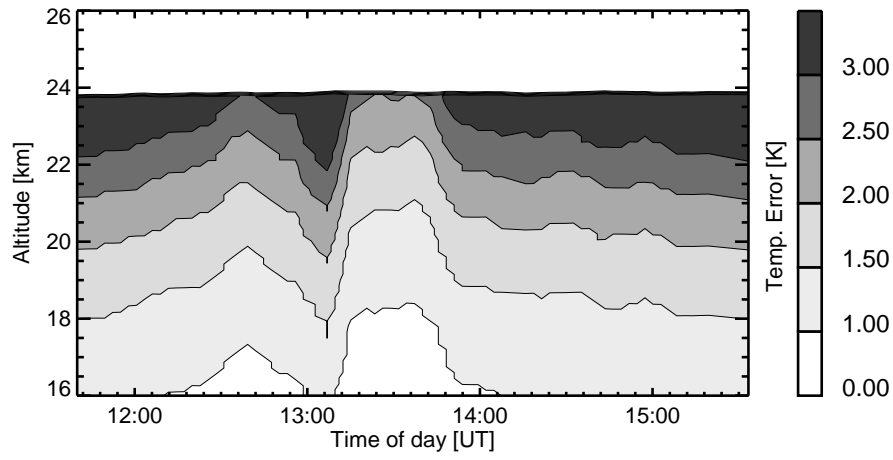
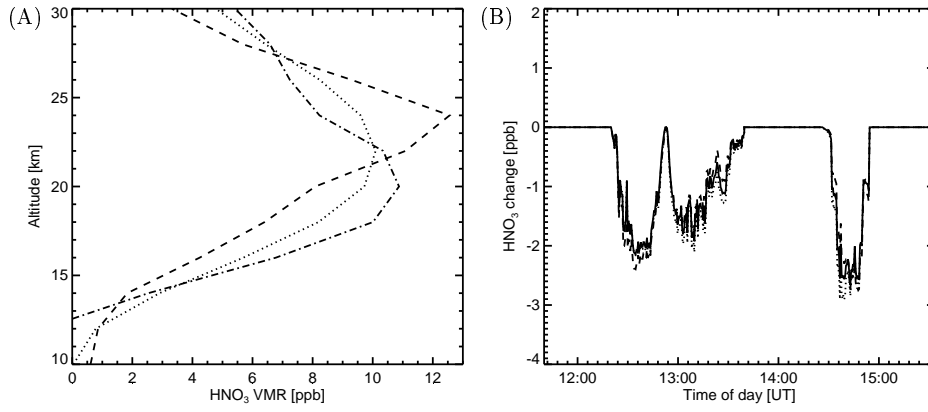
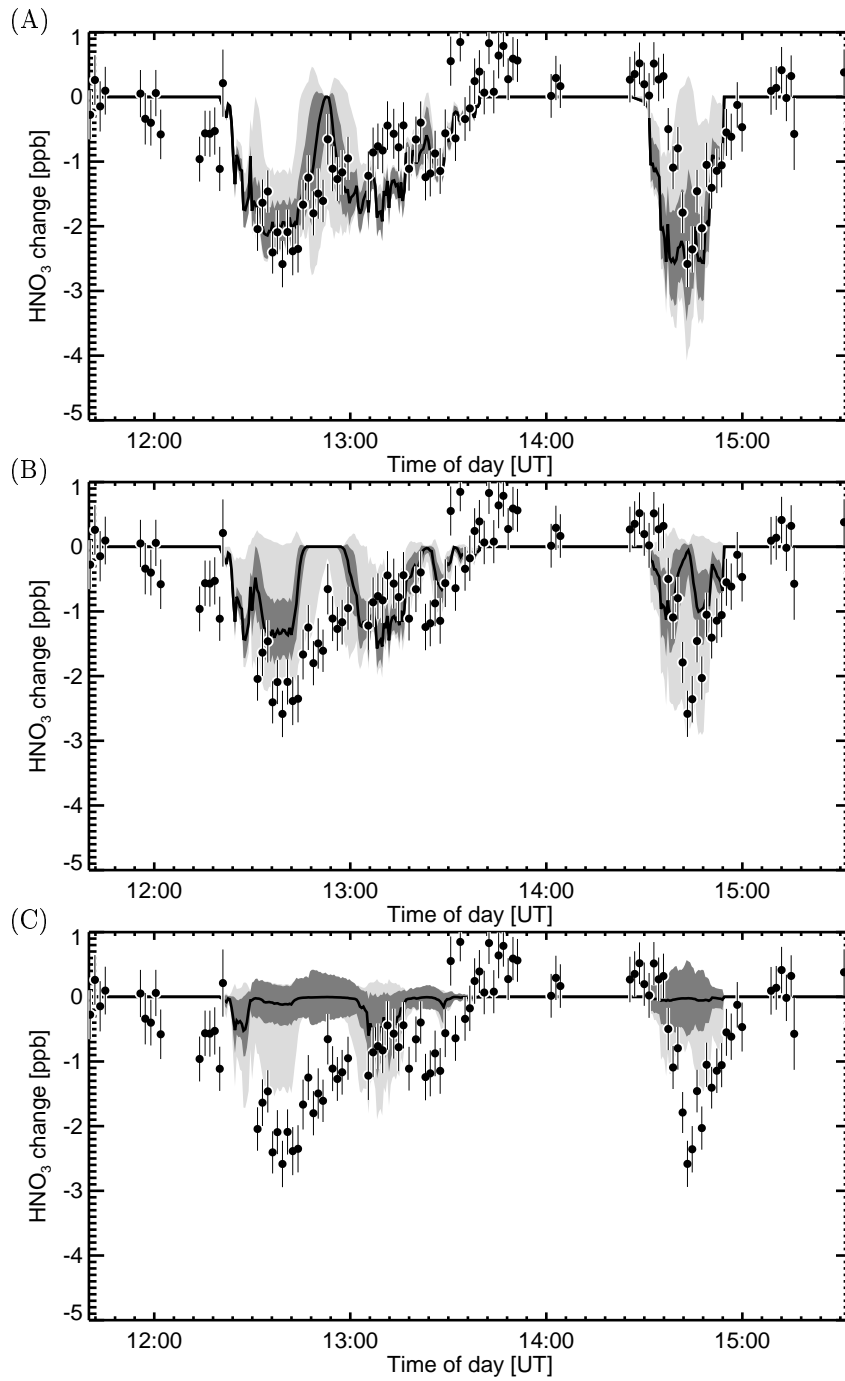


Figure 5. Uncertainty of the AROTEL temperature data along the flight-path of the DC-8



**Figure 6.** The sensitivity of the model results to the vertical resolution of total HNO<sub>3</sub>. Left: three HNO<sub>3</sub> profiles with different peak altitudes, peak values and peak width, but similar column amounts. All three profiles yield the total HNO<sub>3</sub> profile used for the model calculations when smoothed to the ASUR vertical resolution. Right: Model runs for the case of a NAT composition for the three HNO<sub>3</sub> profiles shown in the left-hand plot at 22 km altitude.



**Figure 7.** Model sensitivity for NAT (top), NAD (middle) and STS (bottom), for 22 km altitude. Lines correspond to the model base results (see Figure 4). Light grey area: total model errors considering errors in temperature, water vapor, total HNO<sub>3</sub> and H<sub>2</sub>SO<sub>4</sub> (the latter for STS only). Dark grey area: the same, but without the contribution of temperature errors. Black dots and error bars as in Figure 4.

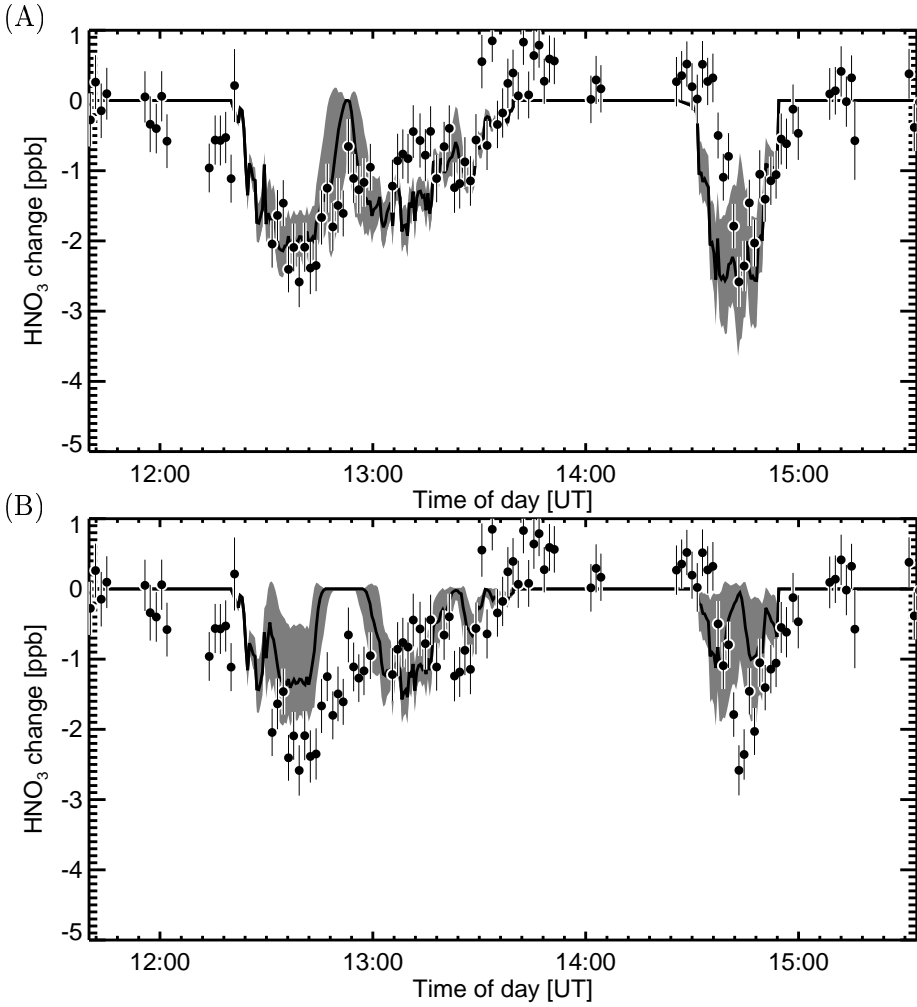


**Figure 8.** Model errors for NAT (top) and NAD (bottom) assuming a temperature uncertainty of 1 K. Grey area: Model errors. Symbols, lines and error bars as in Figure 4.

**Table 1.** Parameters used for the modeling of gas-phase  $\text{HNO}_3$  and their assumed uncertainties.

Parameter	Value/source	Uncertainties
Temperature	AROTEL	see Figure 5
$\text{H}_2\text{O}$	4.75-6.25 ppm <sup>a</sup>	1 ppm
total $\text{HNO}_3$	ASUR <sup>b</sup>	15 %
$\text{H}_2\text{SO}_4$	0.5 ppb <sup>c</sup>	0.3-1.1 ppb

<sup>a</sup>Altitude dependent.

<sup>b</sup>Total  $\text{HNO}_3$  is derived from ASUR measurements of the same day, but without PSC coverage.

<sup>c</sup>From [Beyerle et al., 1997]